VOL. 16, NO. 19, OCTOBER 2021 ISSN 1819-6608
ARPN Journal of Engineering and Applied Sciences

www.arpnjournals.com

THERMAL-HYDRAULIC PROCESSES IN AIR AND CARBON DIOXIDE GAS TURBINES

Kindra V., Komarov I., Osipov S., Makhmutov B. and Naumov V.
Department of Innovative Technologies for High-Tech Industries, Moscow Power Engineering Institute, Moscow, Russia
E-Mail: kindra.vladimir@yandex.ru

ABSTRACT

The continuous increase of the anthropogenic emission of carbon dioxide and toxic agents causes the development of oxy-fuel combustion power cycles. This development involves the improvement of the advanced approach to the design of the carbon dioxide operating power production equipment. This paper discloses the influence of the thermodynamic and thermal-physical performance of gas turbine cooling agents upon the efficiency of the thermal-hydraulic process in the flowpath and cooling system channels.

Keywords: thermal-hydraulic, flat wall temperature, oxy-fuel combustion power cycles.

INTRODUCTION

The currently solved problem of carbon oxides emission in the power production industry emphasizes the development of closed thermodynamic cycles with oxy-fuel combustion [1, 2]. The best-known research papers are [3-8]. The comparison of oxy-fuel combustion power cycles shows that one of the prospective technologies is the Allam cycle that operates the carbon dioxide CO2 with supercritical parameters [9].

The cycle authors claim its net efficiency of 58.9% on natural gas and 51.44% on coal including the carbon dioxide storage. Paper [9] assesses a very low specific cost of this technology, which is $ 800–1000/kW on natural gas and $ 1500-1800/kW on coal gasification gas. This may be compared with $ 5000/kW for the modern combined cycle power plants with internal gasification [10]. This low installed power price for the Allam cycle is due to the compact power plant and main equipment that is achieved by a drastic pressure increase in the low potential part of this cycle.

New cycles with non-traditional working fluids require new types of main and auxiliary power production equipment. The concerning technical problems are related to the choice of equipment type and manufacturing materials and development of new methods for design, manufacturing, mounting, and operation.

The development of the new Allam cycle turbine is of special importance. The first experience in this turbine design and manufacturing belongs to the 50 MW Toshiba. Some of the key features of the turbine buildup are disclosed in [9]. If its operation will be successful the plan is to develop an over 300 MW turbine.

The design of 300-400 MW turbines on supercritical carbon dioxide is disclosed in the papers [11, 12]. These papers emphasize the importance of the heat carrier verification for the design of the hot parts cooling system.

This paper investigates approaches to the development of the blade cooling system for high temperature turbine operating on carbon dioxide. The approach involved the solution of the following problems:

- Influence of type and thermodynamic performance of the gas turbine working fluid upon the thermo-hydraulic process efficiency.
- Influence of type and thermodynamic performance of the gas turbine cooling agent upon the thermo-hydraulic process efficiency.
- Influence of the gas turbine blade wall thickness upon the temperature drop.

RESEARCH OBJECT

Analysis of type and thermodynamic performance of the gas turbine working fluid and cooling agent upon the thermo-hydraulic process efficiency was carried out for the following thermodynamic cycles:

- Allam cycle on carbon dioxide with the inlet (inlet pressure p_0, inlet temperature t_0) and outlet (outlet pressure p_{out}, outlet temperature t_{out}) parameters of 30 MPa, 1083°C and 3 MPa, 720°C respectively; these parameters provide the maximal thermodynamic cycle efficiency [13].
- Gas turbine Brayton cycle with air as the main component of the working fluid and the initial and final parameters of 1.15 MPa, 1060°C and 0.1 MPa, 537°C respectively; the example gas turbine is GTE-160 by Power Machines-Siemens.

The gas turbine cycle initial and final temperatures are close to the Allam cycle ones but its initial and final pressures are remarkably lower (Table-1). In the gas turbine Brayton cycle the working fluid is the combustion product but its initial parameters are not high so the analysis involves air for the cycle working fluid.

The initial approach to the analysis of high temperature carbon dioxide turbine cooling is a thermo-hydraulic investigation of a plate. The plate may be surrounded by a heat carrier flow of air or carbon dioxide. The analysis considers a steady flow of different fluids around a 140 mm long plate (Figure-1). The thermo-hydraulic analysis results shows the cooling system efficiency and recommends an approach to the system design. The plate is taken for the analysis because any of the turbine flowpath surfaces may be presented as a sequence of small plates. Besides, this approach eliminates

the influence of blade surface curvature effect upon the analysis results.

Table-1. Working fluid parameters assumed for the analysis of the cycles.

Cycle	Working fluid	p_0, MPa	t_0, °C	p_{out}, MPa	t_{out}, °C
Allam	Carbon dioxide	30	1083	3	720
Brayton	Flue gas	1.15	1060	0.1	550

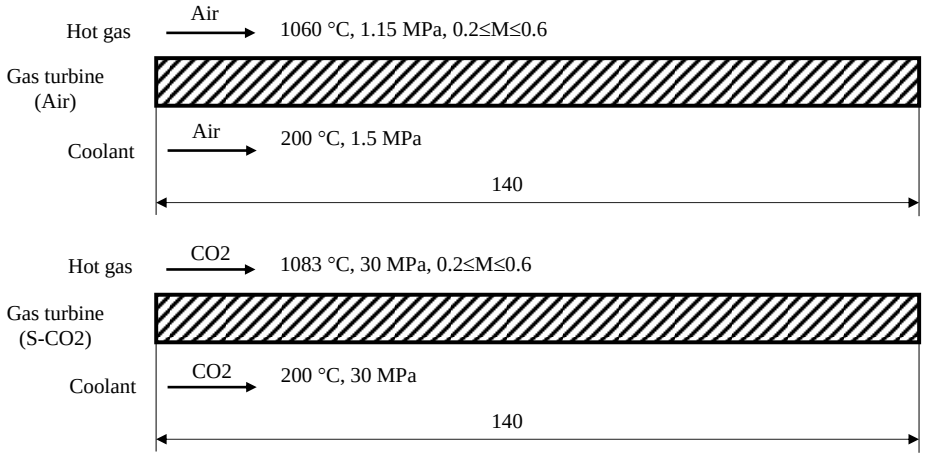

Figure-1. The comparison of thermal-hydraulic characteristics of the flat plane for air and carbon dioxide flows at different thermodynamic parameters.

METHODOLOGY

The flow analysis problem is solved in a 1-D approach. The plate temperature is assumed as 850°C that corresponds to the maximal acceptable blade metal temperature [13]. The flow conditions correspond to the air and supercritical carbon dioxide turbine inlet conditions. The turbine operating range is the Mach number from 0.2 to 0.6 which is similar to inter-airfoil flow in the turbine inlet guide vane.

The main thermo-hydraulic performance of the plate is determined according to [14]. The local value of Nusselt number for laminar boundary layer is defined as follows (1):

$$\mathrm{Nu}_x = 0.032 \cdot \mathrm{Re}_x^{0.5} \cdot \mathrm{Pr}_\infty^{\frac{1}{3}} \cdot \left(\frac{\mathrm{Pr}_\infty}{\mathrm{Pr}_w}\right)^{0.25}, \quad (1)$$

where Nu_x - local Nusselt number; $\mathrm{Re}_x = U_\infty \cdot x/\nu$ - local Reynolds number; x - plate axial coordinate; ν - fluid kinematic viscosity; Pr_∞ - Prandtl number at flow temperature; Pr_w - Prandtl number at wall temperature.

The local Nusselt number for the turbulent boundary layer is determined as follows (2):

$$\mathrm{Nu}_x = 0.0296 \cdot \mathrm{Re}_x^{0.8} \cdot \mathrm{Pr}_\infty^{0.4} \cdot \left(\frac{\mathrm{Pr}_\infty}{\mathrm{Pr}_w}\right)^{0.25}, \quad (2)$$

The laminar and turbulent boundary layers friction coefficients are calculated with the equations (3) and (4):

$$C_f = \frac{0.664}{\sqrt{\mathrm{Re}_x}}. \quad (3)$$

$$C_f = \frac{0.0592}{\mathrm{Re}_x^{0.2}}. \quad (4)$$

For calculating the wall temperature following approach was used. In the text below the working fluid and cooling agent are assigned with the indexes are *1* and *2* for respectively.

The heat flux from working fluid to coolant through the flat wall is defined as follows (5):

$$q = \frac{T_{\mathrm{hc1}} - T_{\mathrm{hc2}}}{\frac{1}{\alpha_1} + \frac{\delta}{\lambda_w} + \frac{1}{\alpha_2}}, \quad (5)$$

where λ_w - heat conductivity of the wall; α_1 - heat transfer coefficient for the first heat carrier, α_2 - heat transfer coefficient for the second heat carrier; T_{hc1} - temperature of the first heat carrier; T_{hc2} - temperature of the second heat carrier.

Along the flat plate length, the mean Nusselt number values for the turbulent flow with constant parameters are defined as follows (6):

$$\overline{\mathrm{Nu}} = 0.037 \cdot \mathrm{Re}^{0.8} \cdot \mathrm{Pr}_\infty^{0.4} \cdot \left(\frac{\mathrm{Pr}_\infty}{\mathrm{Pr}_w}\right)^{0.25}. \quad (6)$$

The wall temperatures on the working fluid and coolant sides are given by the Newton–Richman law (7):

$$q = \alpha \cdot (T_{hc} - T_w), \quad (7)$$

where T_{hc} – heat carrier temperature; T_w – plate surface (wall) temperature.

The wall temperature distribution may be obtained by a solution of the heat transfer differential equation (8):

$$\frac{d}{dx}(\lambda \frac{dT}{dx}) = 0,$$
$$T(x=0) = T_{w1}, T(x=\delta) = T_{w2}, \quad (8)$$
$$T = T_{w1} + \frac{T_{w2} - T_{w1}}{\delta} \cdot x,$$

where x - transverse coordinate.

INFLUENCE OF TYPE AND THERMODYNAMIC PERFORMANCE OF THE GAS TURBINE WORKING FLUID UPON THE THERMO-HYDRAULIC PROCESS EFFICIENCY

Thermo-hydraulic parameters for the one side of the plate blown by two types of fluids are shown in Figure-2. The transition from air to carbon dioxide remarkably increases the plate heating intensity (Figure-2a). Specifically, at Mach number M=0.6 the ratio of carbon dioxide and air Nusselt numbers is equal to 15. The source of this intensive carbon dioxide heat transfer is its 30 times higher Reynolds number at equal Mach numbers. This is mostly caused by the 37 times lower carbon dioxide kinematic viscosity at the given parameters that that of air.

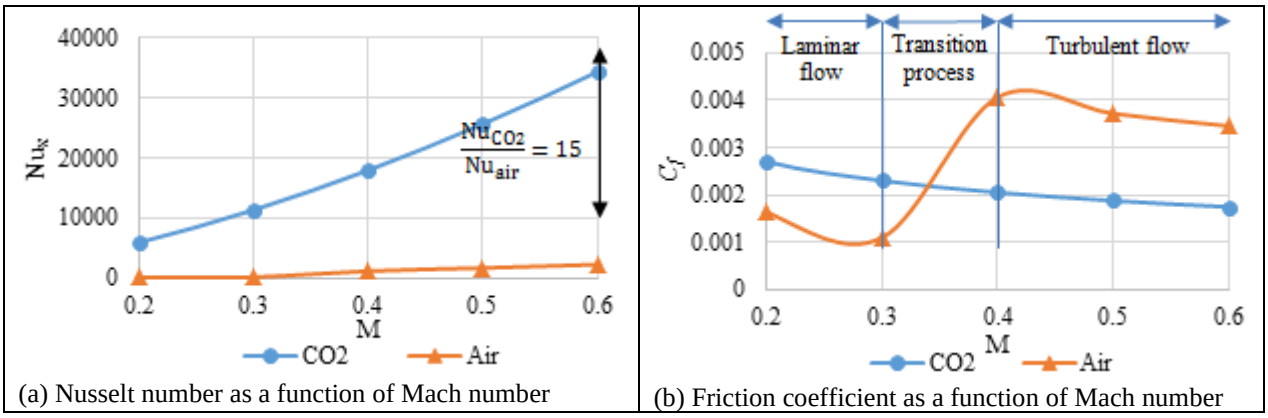

(a) Nusselt number as a function of Mach number

(b) Friction coefficient as a function of Mach number

Figure-2. The comparison of Nusselt number and flow friction coefficient for the gas turbine working fluid conditions.

Figure-2b shows the friction coefficient versus Mach number for the air flow with three specific parts. The first part with 0.2<M<0.3 is laminar. The second part with 0.3<M<0.4 is a transition. The third part with M>0.4 is turbulent. In the turbulent boundary layer, the air flow has a higher friction coefficient than the carbon dioxide which is also caused by the higher Reynolds numbers in carbon dioxide. At equal Mach numbers, the transition from air to carbon dioxide reduces the friction coefficient by about 50%.

INFLUENCE OF THE COOLING AGENT PARAMETERS UPON THE GAS TURBINE EFFICIENCY

The next stage of analysis consists of thermal and aerodynamic studies at flow parameters corresponding to the power facility ones. The flow around the plate consists of air or supercritical carbon dioxide. Similar calculations of the coolant flow local Nusselt numbers and friction coefficients are presented in Table-2.

Table-2. Thermal-physical performance and operation parameters of the air and carbon dioxide gas turbine coolants.

Thermal-physical performance and operation parameters	Coolant	
	CO2	Air
Pressure p, MPa	30	1.5
Inlet flow temperature T, °C	200	200
Sound velocity a, m/s	376.22	437.77
Kinematic viscosity $v \cdot 10^8$, m^2/s	9.089	238
Prandtl number Pr	1.047	0.702
Heat conductivity λ, W/(m·K)	0.0516	0.0317

Figure-3a data show that the plate cooling with carbon dioxide is more efficient than air cooling. At the Mach number of 0.6, the ratio of Nusselt numbers for carbon dioxide and the air is about 14. The transition of the cooling agent from air to supercritical carbon dioxide at M=0.6 reduces the friction coefficient by about 50% (Figure-3b).

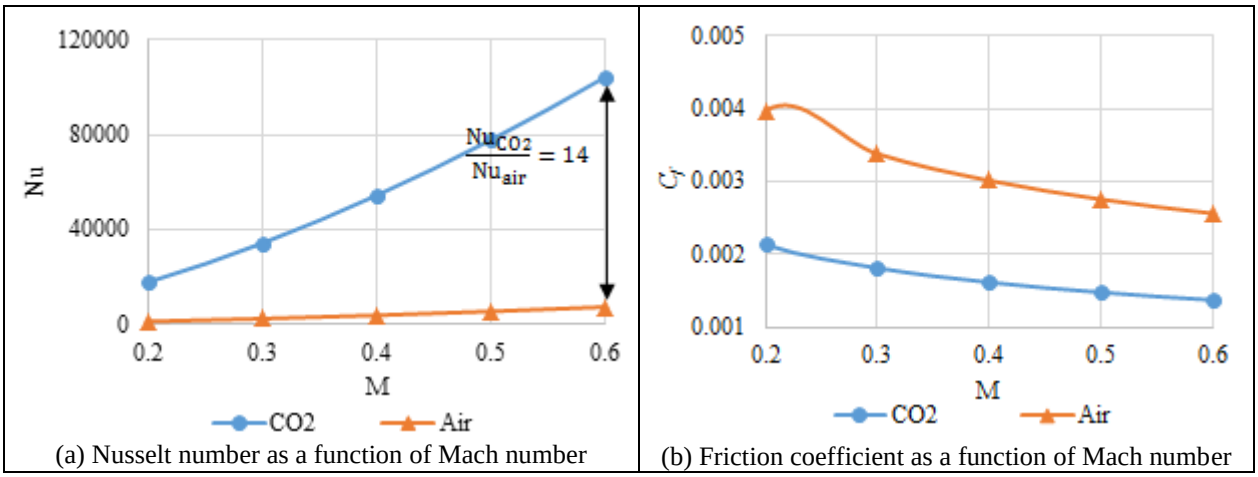

(a) Nusselt number as a function of Mach number

(b) Friction coefficient as a function of Mach number

Figure-3. The comparison of Nusselt number and flow friction coefficient for the gas turbine coolant conditions.

For both cooling agents at all Mach number values and the given flow parameters, the ratio of local Nusselt numbers on the coolant side is above 1. Thus, in both cooling agents, the plate cooling is more efficient than its heating. For the CO2 coolant, the Nusselt number ratio from the coolant to the working fluid is about 3 in the whole range of Mach number. For the air coolant, this ratio has a maximum at M≈0.3. This effect may be explained by the occurrence of a laminar flow layer in the hot side flow where the local Nusselt number is lower than on the coolant side at equal Mach numbers.

At Mach numbers below 0.4, the friction coefficients ratio on hot and cold sides for carbon dioxide is smaller than that for air. At higher Mach numbers the carbon dioxide and air friction coefficients are about equal.

Thus, the analysis shows that at the moderate pressure of about 1 MPa the transition from air to carbon dioxide coolant provides the local Nusselt number grow on both hot gas and coolant sides. This produces a remarkable temperature difference on the plate sides and the related plate thermal stresses. Thus, the high temperature gas turbine blade walls will be subject to high thermal stress.

Due to an increase in the influence of plate heat resistance on the heat transfer process, it is necessary to analyze the impact of plate width on the temperature difference.

INFLUENCE OF BLADE WALL THICKNESS UPON ITS TEMPERATURE DIFFERENCE

The coolant and working fluid types influence the plate surfaces temperature difference. This stage of analysis assumed the plate thickness of 2, 4, and 6 mm which are compatible with the gas turbine blade wall thickness, the plate length 140 mm was equal to the previous study. The plate materials heat conductivity was assumed as equal to the KhN65VMTYu heat resistant nickel alloy at *T*=850°C.

Velocities of both flows are assumed 100 m/s which are compatible with the gas turbine first stage inter-blade channel velocity. The working fluid and coolant thermodynamic parameters are assumed equal to the gas turbine and cooling channel inlets respectively (Tables 2 and 3).

The Reynolds number values on the coolant side are determined by the maximal acceptable wall temperature on the hot gas side at the given plate thickness. At this condition, the temperature drop will be maximal because the hot side temperature is fixed as maximal acceptable.

Table-3 summarizes the Reynolds number values for the two heat carriers at various plate thicknesses.

Table-3. Reynolds number values for the two fluids and different wall thicknesses.

Material	δ, mm	Reynolds number
CO2	2	1 800 000
CO2	4	2 280 000
CO2	6	2 940 000
Air	2	1 240 000
Air	4	1 580 000
Air	6	1 760 000

Figure-4 shows the wall temperature distributions at carbon dioxide flows on hot and cold sides. The Reynolds number values on the coolant side are taken from Table-4. Similar relations for air are shown in Figure-5.

The relations in Figures 4 and 5 show larger temperature drops with CO2 flow than with the air one. This effect is caused by larger coolant side Reynolds number values in CO2 which results in more intensive heat transfer and better wall cooling. Here the flow conditions on the working fluid side are fixed.

The next stage is a calculation of the coolant side Reynolds number that provides the acceptable wall temperature on the hot gas side for the two coolant types at different wall thicknesses (Figure-6).

Figure-6 shows that the acceptable wall temperature may be provided by lower coolant Re numbers with air than with carbon dioxide. Thus at equal Reynolds number values for the two coolants the air cooling requires lower coolant flow (Figure-7). This effect improves the thermodynamic cycle efficiency. It is worth mentioning that the coolant flow difference is larger at larger Reynolds number. At equal specific dimensions and Re=80 000 the carbon dioxide flow is about 35% higher than that of the air one. The CO2 flow at the constant Reynolds number value may be reduced by an increase of the cooling channel specific dimension from the air one.

Temperature drop between the plate surfaces in Figure-8 shows that the needed drop with air and carbon dioxide may be reached at different wall thicknesses. For example, the 150°C temperature drop may be reached at 6 mm wall thickness in air flow and 3 mm thickness in CO2 flow. In the considered range of plate thickness, the temperature drop above 150°C may be reached only in the carbon dioxide flow.

It is worth mentioning that the wall thickness needed for the given temperature drop may be limited by the reliability and strength requirements. This leads to a conclusion of the necessary heat transfer increase on the coolant side. This heat release on the coolant side may be improved by the application of flow turbulators or by an increase of Reynolds number.

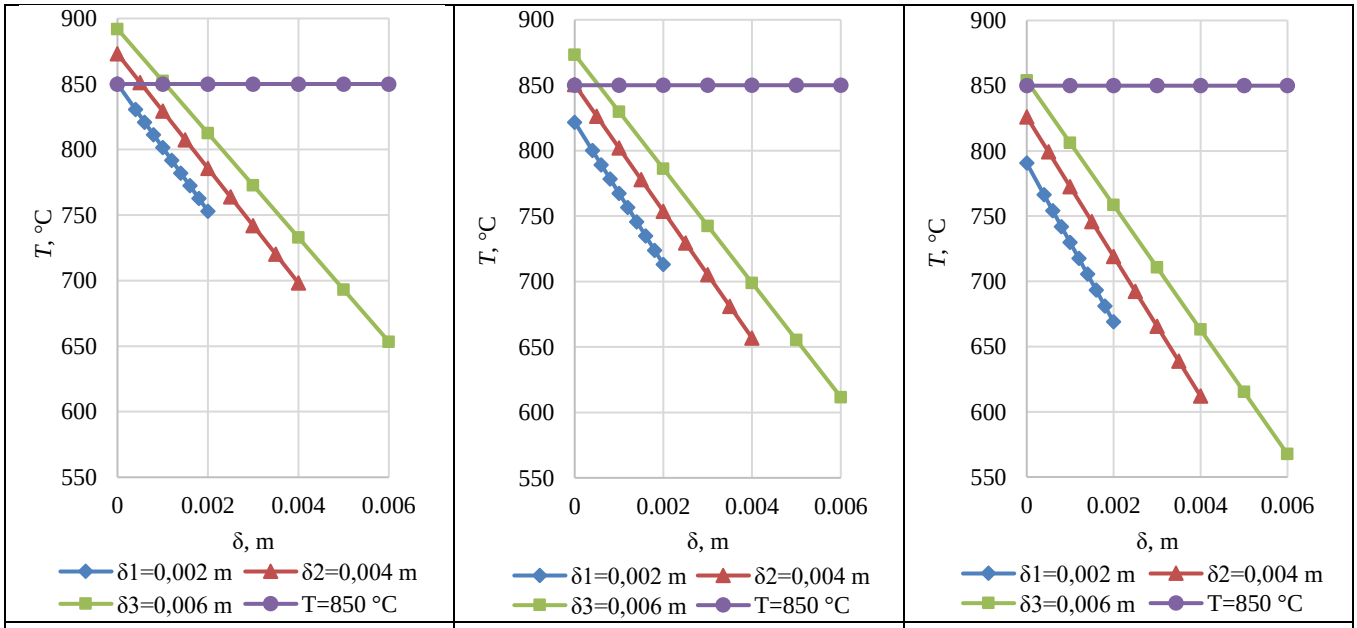

(a) Re_x=1 800 000 (b) Re_x=2 280 000 (c) Re_x=2 940 000

Figure-4. Flat wall temperature distribution at carbon dioxide flows on hot and cold sides.

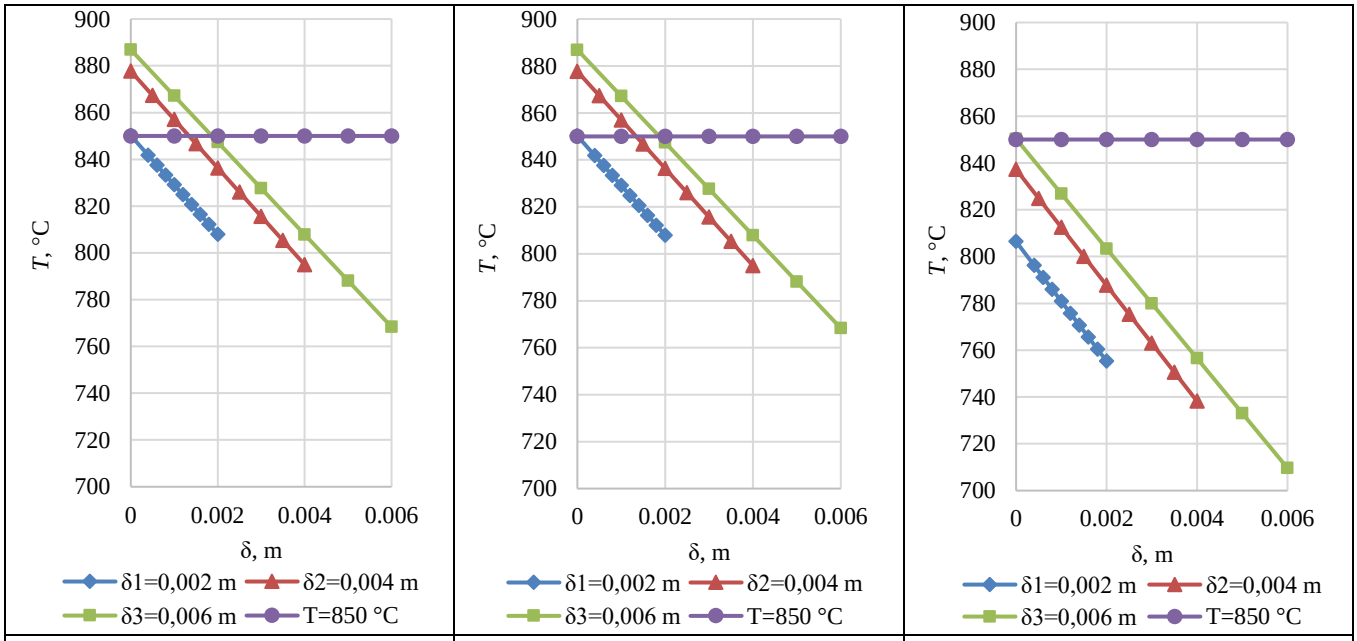

(a) Re_x=1 240 000 (b) Re_x=1 580 000 (c) Re_x=1 760 000

Figure-5. Flat wall temperature distribution at air flows on hot and cold sides.

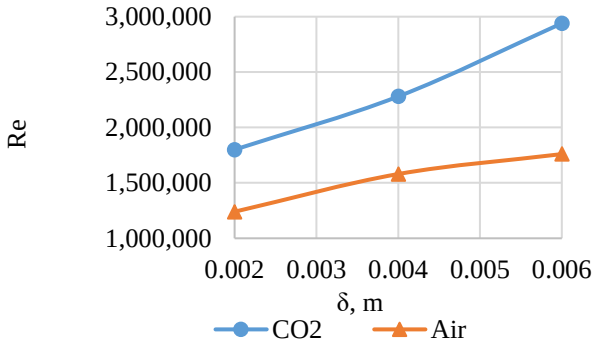

Figure-6. Coolant Re number values vs plate thickness.

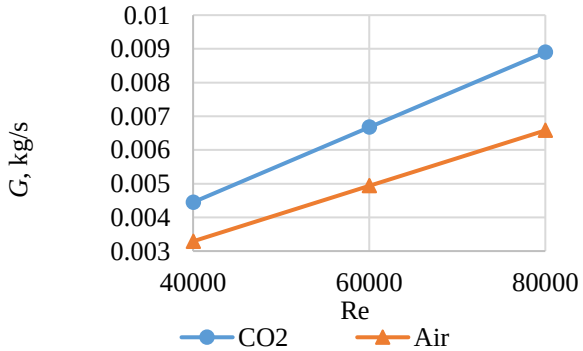

Figure-7. Coolant flow that provides needed blade cooling vs Reynolds number.

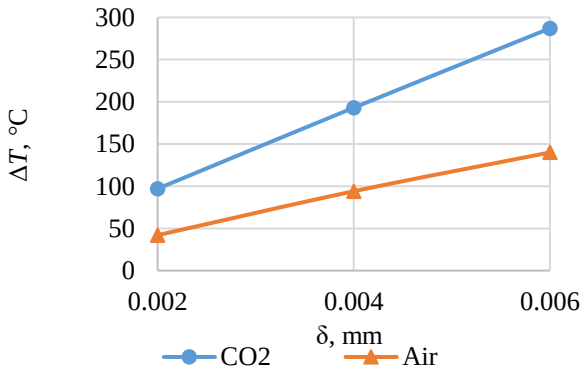

Figure-8. Temperature drop vs plate thickness.

CONCLUSIONS

a) The significant increase of Nusselt number for coolant (14 times) and hot gas (15 times) with the transition from air to CO2 is observed due to higher Re number (30 times) and lower kinematic viscosity (37 times) values for CO2 at the same Mach numbers. The coefficient of hydraulic resistance decreased by 50%.

b) The significant increase of Nusselt number for hot gas and coolant leads to an increase in temperature difference between internal and external surfaces.

c) A decrease of plate width by 3 times leads to the decrease of a temperature difference between internal and external surfaces by 64% for air and by 58% for CO2.

d) To ensure the same level of the wall temperature the Reynolds number for CO2 should be 67% higher.

ACKNOWLEDGMENTS

This study conducted by Moscow Power Engineering Institute was financially supported by the

Ministry of Science and Higher Education of the Russian Federation (project No. FSWF-2020-0020).

REFERENCES

[1] Rogalev A., Komarov I., Kindra V., Zlyvko O. 2018 Entrepreneurial assessment of sustainable development technologies for power energy sector, Entrepreneurship and Sustainability Issues. 6(1): 429-445.

[2] Rogalev A., Kindra V., Osipov S. 2018. Modeling methods for oxy-fuel combustion cycles with multicomponent working fluid. AIP Conference Proceedings 2047, 020020.

[3] Fioravanti A., Lombardi L., Manfrida G. 1998. An innovative energy cycle with zero CO2 emissions. Proceedings of the 43-rd Gas Turbine and Aeroengine Congress and Exhibition, Stockholm, Sweden.

[4] Mathieu P. 1998. Presentation of an innovative zero-emission cycle for mitigating the global climate change. International Journal Applied Thermodynamics. 1(1-4): 21-30.

[5] Iantovski E., Mathieu P. 1997. Highly efficient zero emission CO2-based power plant, Energ. Convers. Manage. 38, 141-146.

[6] Lozza G., Chiesa P. 2000. Natural gas decarbonization to reduce CO2 emission from combined cycles. Part B: Steam-methane reforming, Proceedings of ASME Turbo Expo 2000: Power for Land, Sea, and Air, Munich, Germany.

[7] Andersen T., Kvamsdal M., Bolland O. 2000. Gas turbine combined cycle with CO2-capture using auto-thermal reforming of natural gas, Proceedings of ASME Turbo Expo 2000: Power for Land, Sea, and Air, Munich, Germany.

[8] Fiaschi D., Lombardi L., Tapinassi L. 2004. The recuperative auto thermal reforming and recuperative reforming gas turbine power cycles with CO2 removal - Part II: The recuperative reforming cycle, J. Eng. Gas Turbine Power. 126(1): 62-68.

[9] Allam R. J., Palmer M. R., Brown G. W. Jr, Fetvedt J., Freed D., Nomoto H., Jones C. Jr. 2013. High efficiency and low cost of electricity generation from fossil fuels while eliminating atmospheric emissions, including carbon dioxide, Energy Procedia. 37, 1135-1149.

[10] Klara J. M., Plunkett J. E. 2010. The potential of advanced technologies to reduce carbon capture costs in future IGCC power plants, Int. J. Greenh. Gas Con. 4(2): 112-118.

[11] Zaryankin A., Rogalev A., Osipov S., Kindra V. 2018. Supercritical carbon dioxide gas turbines for high-power generation, AIP Conference Proceedings 2047, 020026.

[12] Rogalev A., Grigoriev E., Kindra V., Rogalev N. 2018. Thermodynamic optimization and equipment development for a high efficient fossil fuel power plant with zero emissions, J. Clean. Prod. 236, 117592.

[13] Pomeroy M. J. 2005. Coatings for gas turbine materials and long term stability issues, Materials and Design. 26(3): 223-231.

[14] Tsvetkov F. F., Grigoryev B. A. 2011. Heat and mass transfer (MPEI, Moscow). p. 562.